

**Supplementary information for:**

**Silicon Nanowire Lithium-ion Battery Anodes with ALD Deposited TiN Coatings Demonstrate a Major Improvement in Cycling Performance**

Alireza Kohandehghan<sup>a</sup>, Peter Kalisvaart<sup>a\*</sup>, Kai Cui<sup>b</sup>, Martin Kupsta<sup>b</sup>, Elmira Memarzadeh<sup>a</sup>, David Mitlin<sup>a, b\*\*</sup>

<sup>a</sup>: University of Alberta Department of Chemical and Materials Engineering, 9107 116th Street, T6G 2V4, Edmonton, AB, Canada.

<sup>b</sup>: National Institute for Nanotechnology (NINT), NRC, 11421 Saskatchewan Dr., Edmonton, AB, T6G 2M9, Canada

\*: [pkalisvaart@gmail.com](mailto:pkalisvaart@gmail.com)

\*\*: [dmitlin@ualberta.ca](mailto:dmitlin@ualberta.ca)

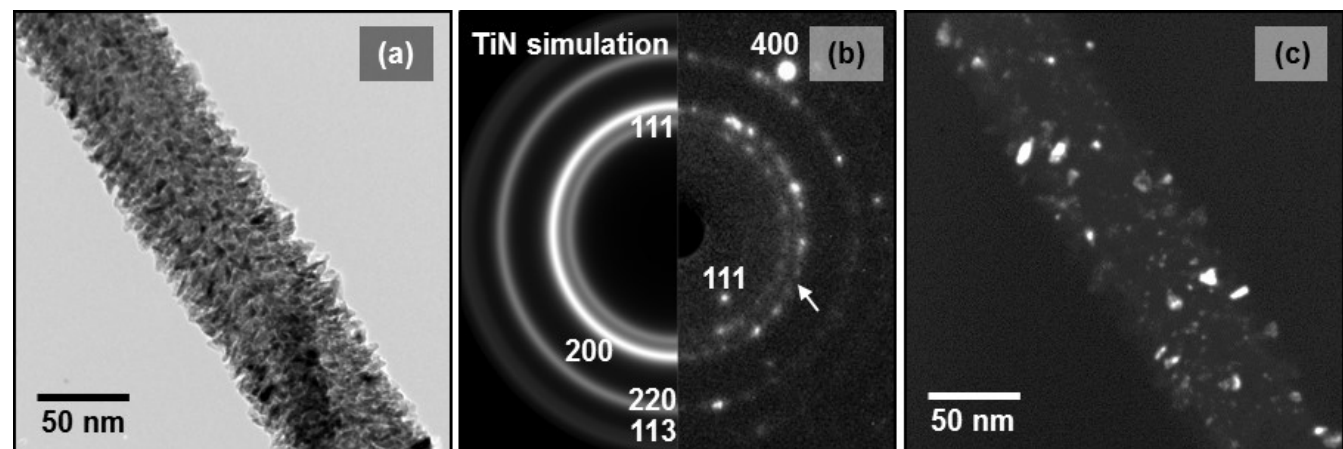


**Fig. S1.** TEM micrographs of Sp15TiN/SiNWs, (a) bright-field micrograph, (b) corresponding indexed SAD pattern with TiN simulation, and (c) dark-field micrograph taken using portion of  $200_{\text{TiN}}$  ring.

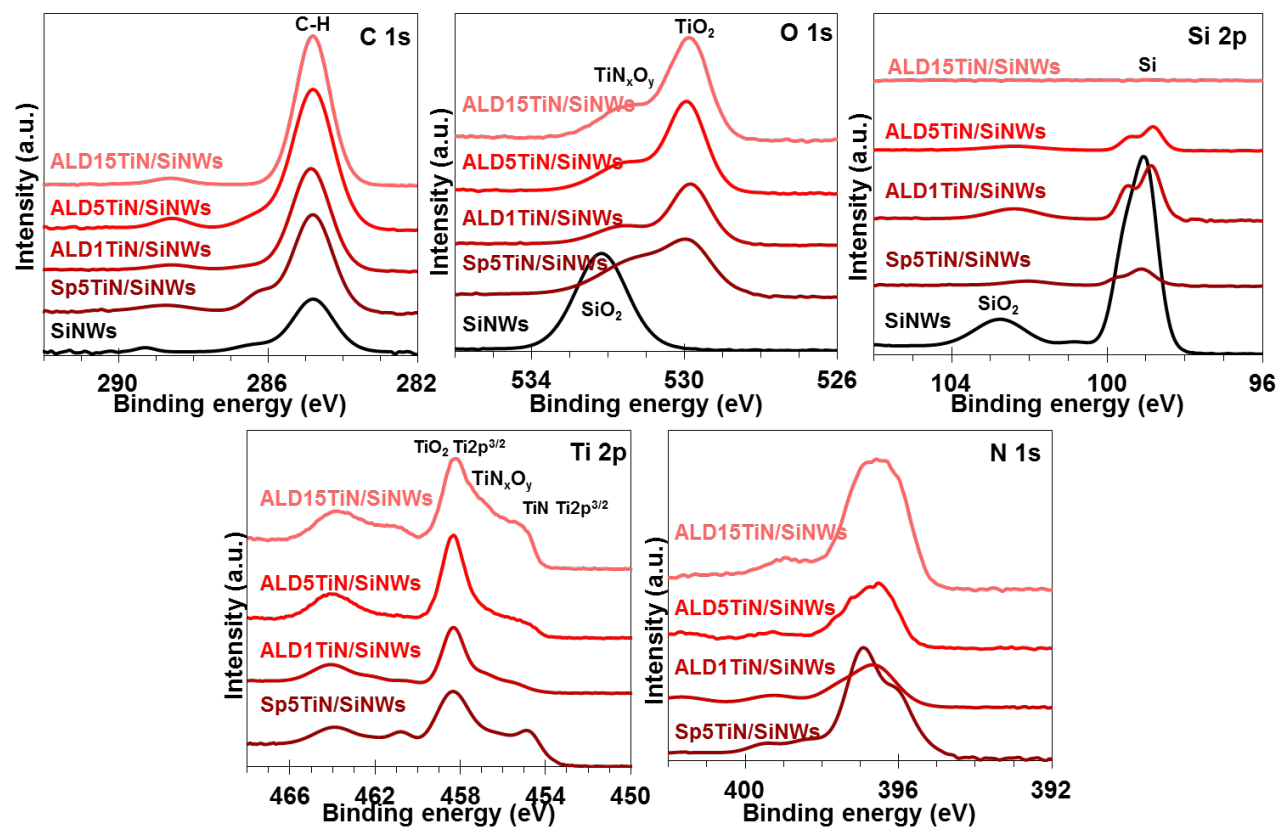


**Fig. S2.** XPS spectra of SiNWs, Sp5TiN/SiNWs, ALD1TiN/SiNWs, ALD5TiN/SiNWs, and ALD15TiN/SiNWs materials in as-synthesized state.

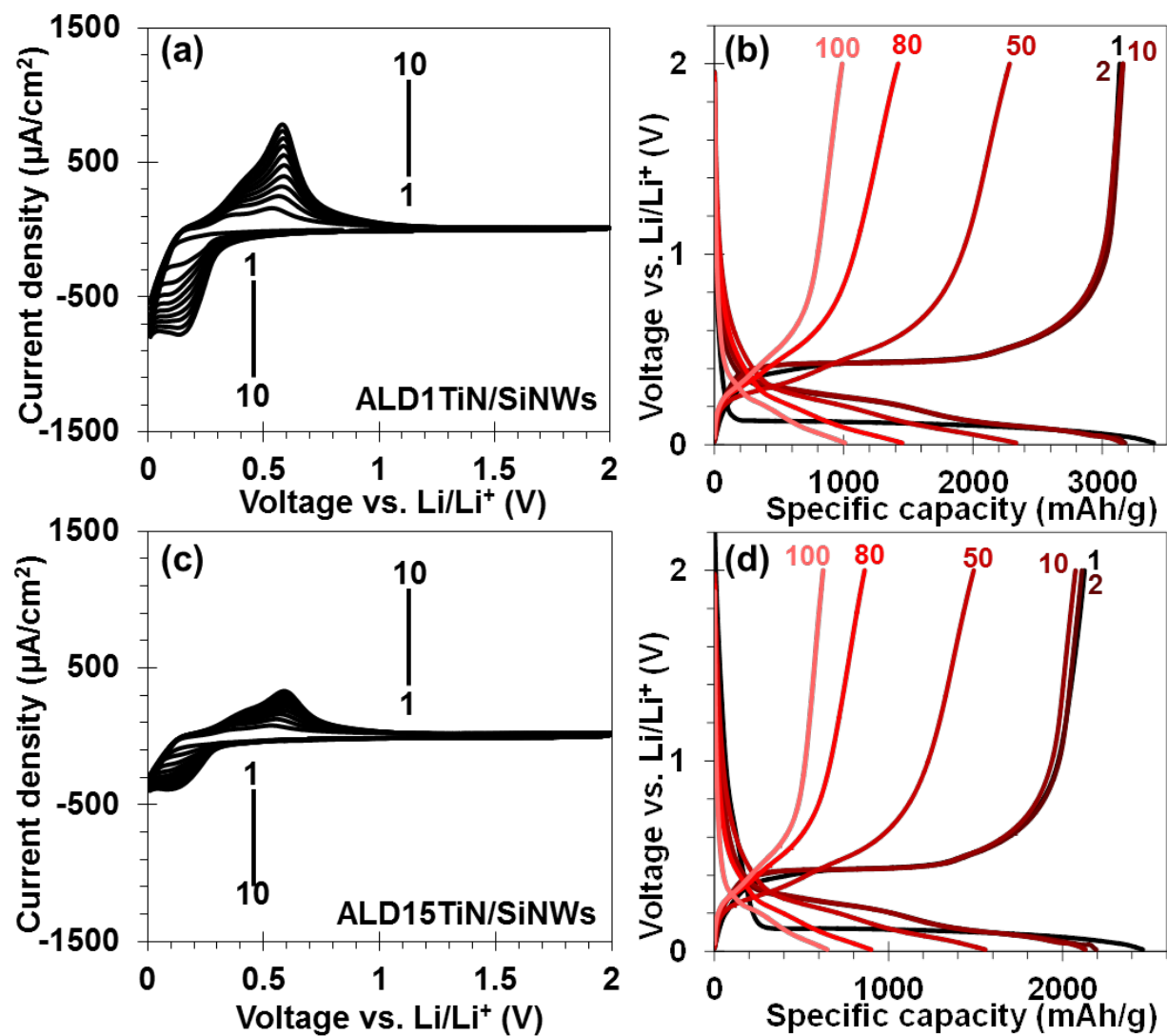


**Fig. S3.** Cyclic voltammetry curves (left column) and galvanostatic voltage profiles (right column) of (a-b) ALD1TiN/SiNWs and (c-d) ALD15TiN/SiNWs.

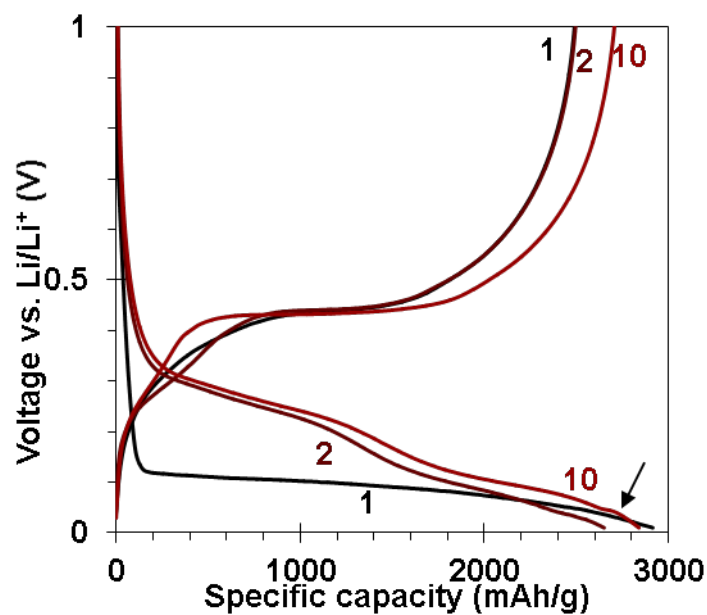


**Fig. S4.** Magnification of cycle 1, 2, and 10 CC voltage profiles for ALD5TiN/SiNWs showing the increase in capacity between cycle 2 and 10 and the small plateau at ~30 mV vs. Li/Li<sup>+</sup> indicated by the arrow, signifying crystallization of Li<sub>15</sub>Si<sub>4</sub>.

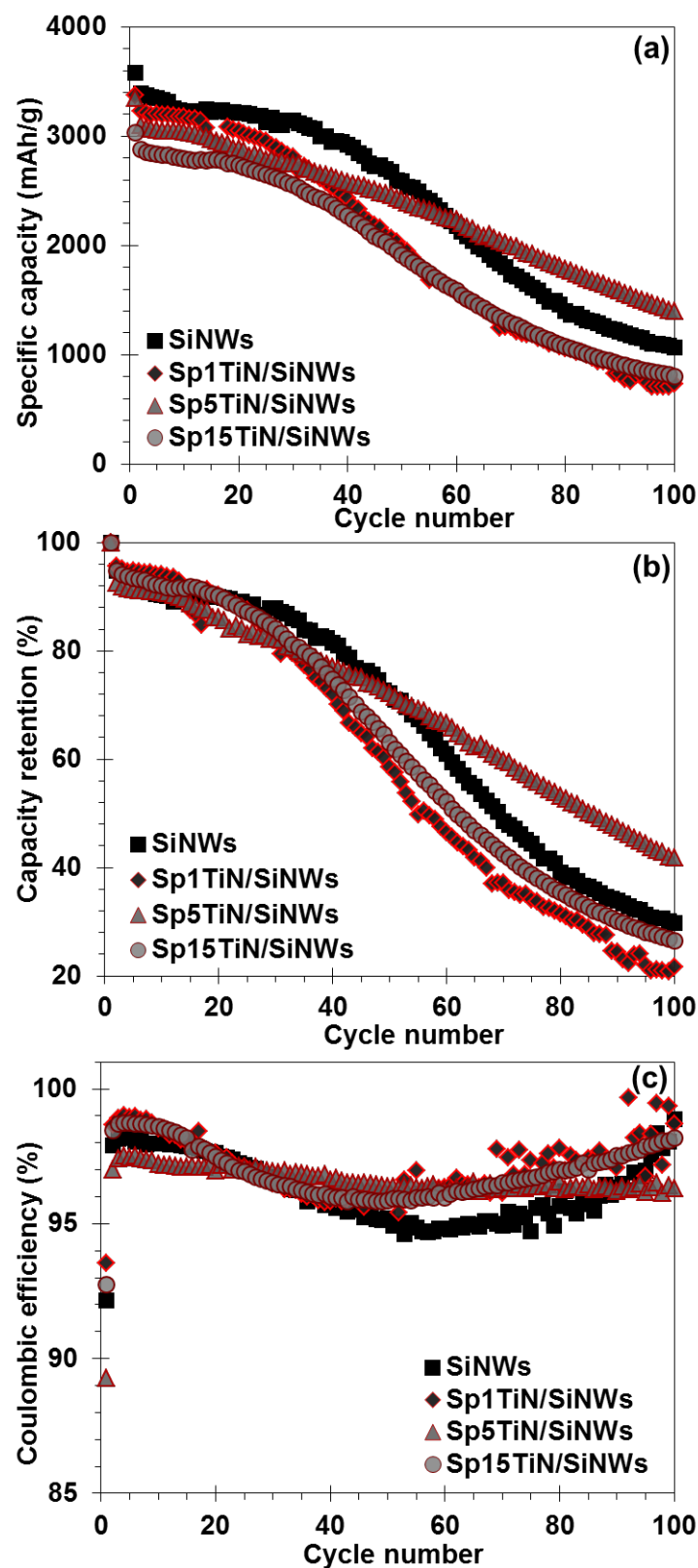


**Fig. S5.** Galvanostatic cycling behavior of SiNWs with sputtered TiN coatings, tested at a rate of 0.1C. (a) Specific capacity retention as a function of cycle number, (b) Capacity retention in % of initial value, and (c) Coulombic efficiency.

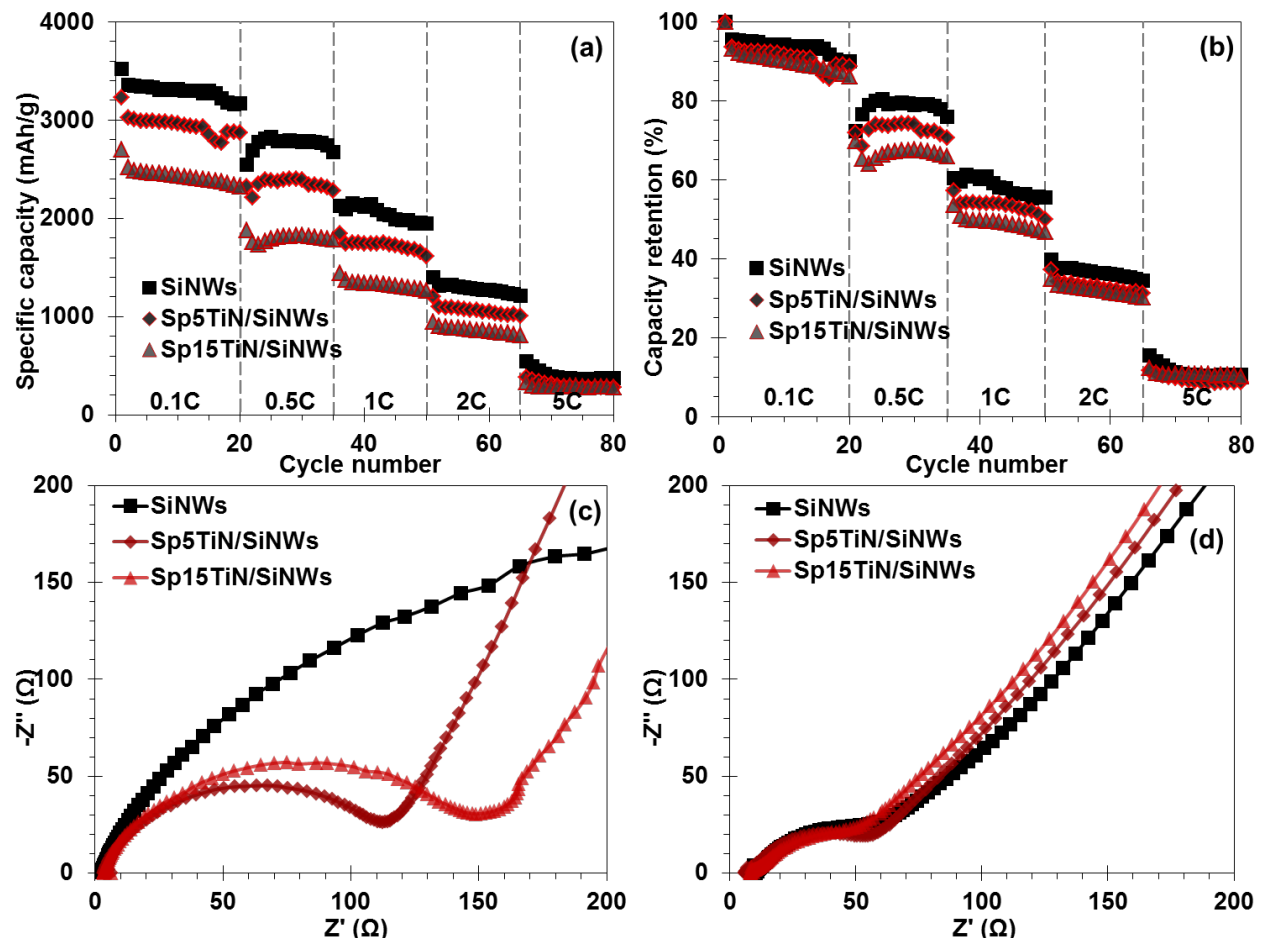


**Fig. S6.** (a-b) Galvanostatic cycling behavior of SiNWs with sputtered TiN coatings, tested at a rates of 0.1C–5C. (a) Specific capacity retention as a function of cycle number, (b) Capacity retention in % of initial value, (c-d) Electrochemical impedance spectra of SiNWs with sputtered coatings, as-synthesized (c) and after 100 cycles (d).

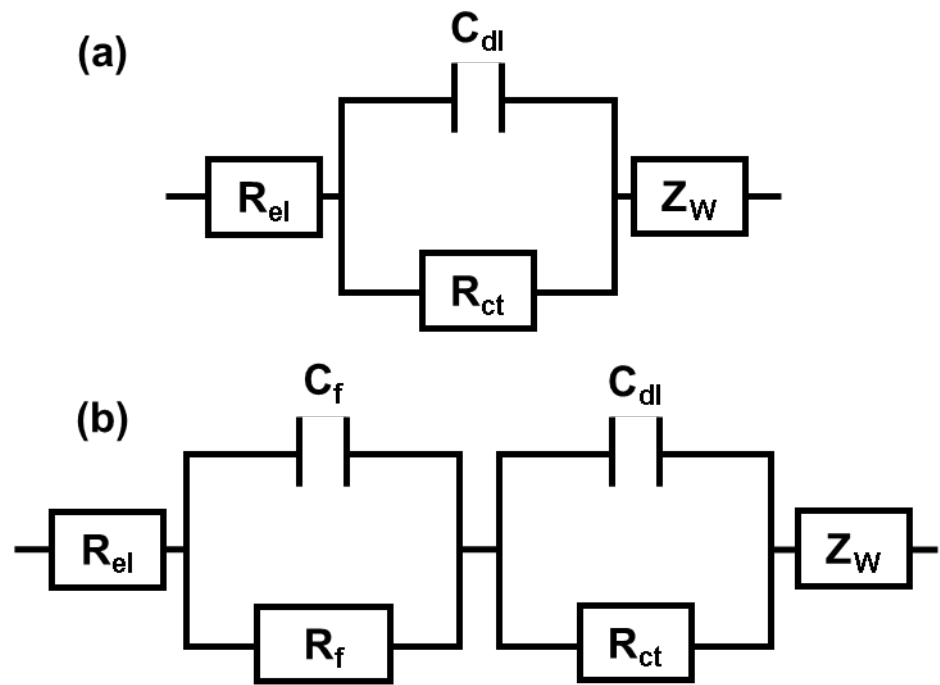


**Fig. S7.** Equivalent electronic circuits used to model the impedance data of as-made (a) and cycled (b) electrodes.

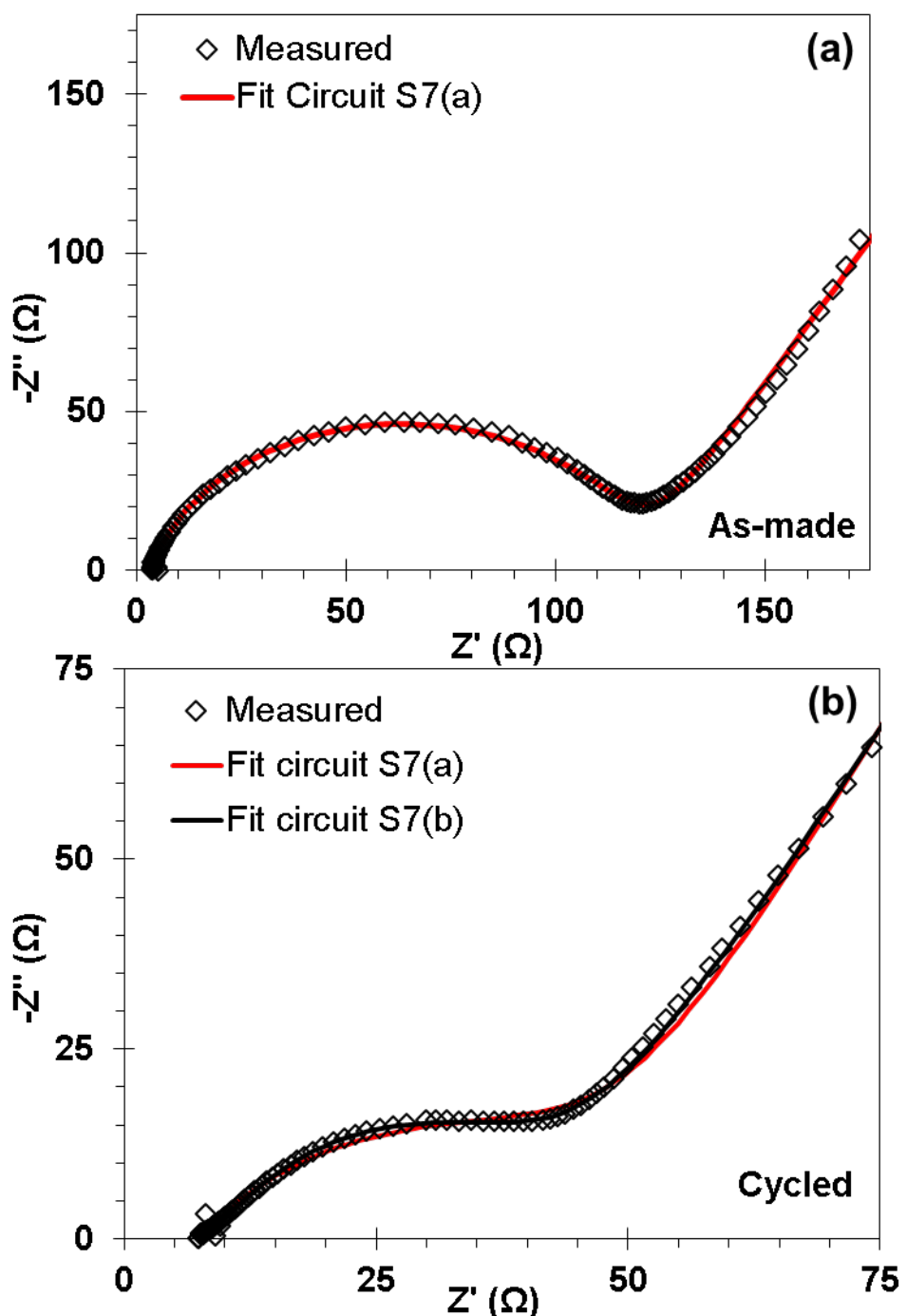


**Fig. S8.** Impedance spectra of ALD1TiN/SiNWs in as-made (a) and cycled state (b) together with simulations based on the equivalent circuits shown in Fig. 7(a) (red line) and Fig. S7(b) (black line). Note that the fit is slightly better using the circuit with 2 time constants, but it is very hard to resolve them.

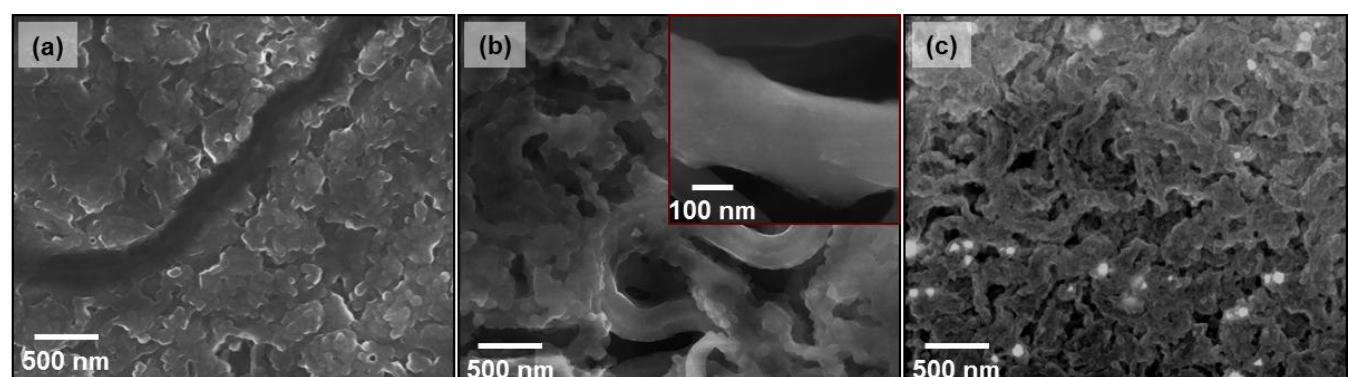


**Fig. S9.** Top-down SEM micrographs of post-100 cycles electrodes; (a) bare SiNWs, (b) ALD5TiN/SiNWs, and (c) ALD15TiN/SiNWs.

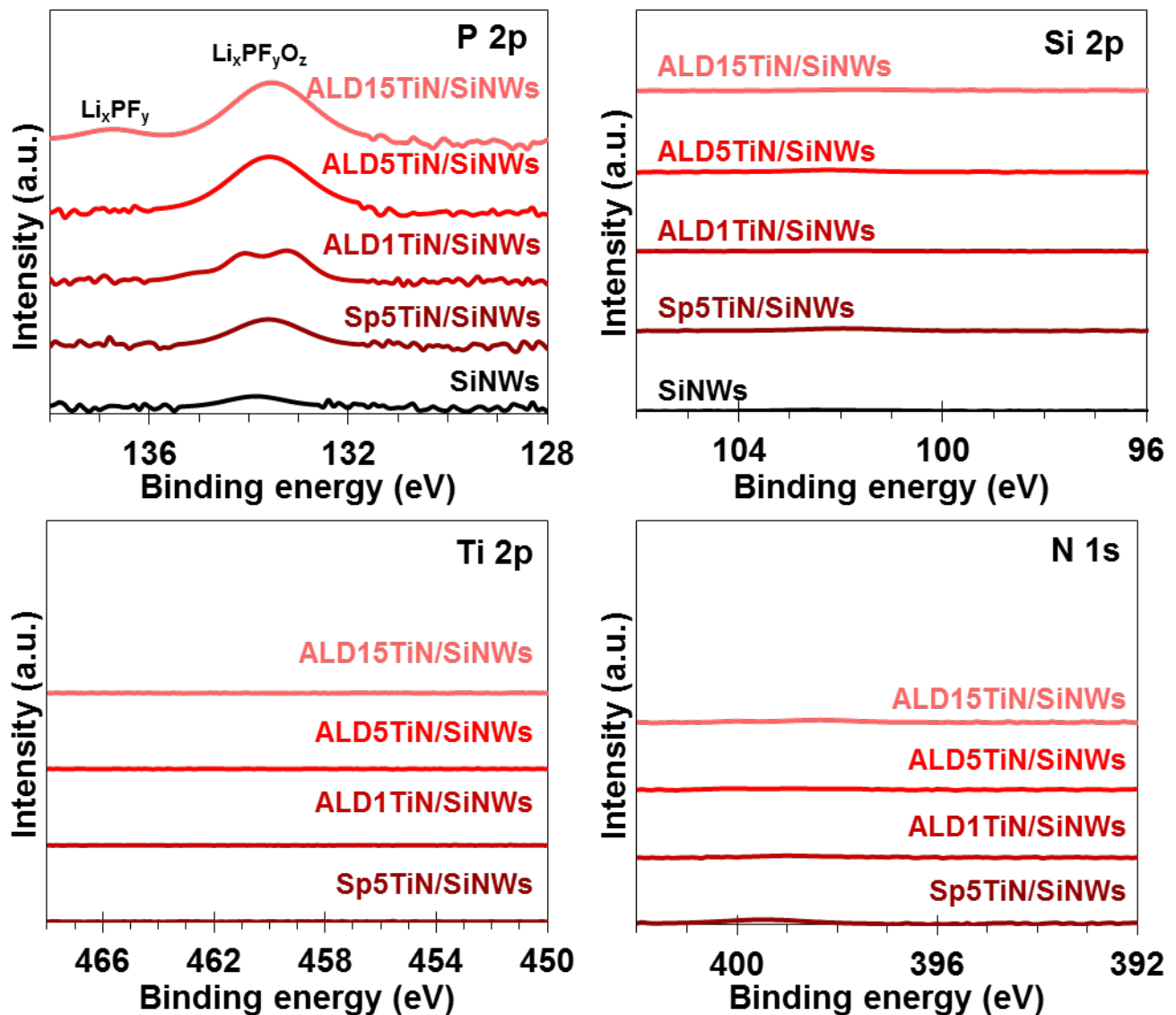


**Fig. S10.** P 2p, Si 2p, Ti 2p, and N 1s XPS spectra after 100 cycles at 0.1C for SiNWs, Sp5TiN/SiNWs, ALD1TiN/SiNWs, ALD5TiN/SiNWs, and ALD15TiN/SiNWs.

**Table S1.** Conductivity of planar TiN films deposited by ALD and sputtering measured by four-point probe.

Deposition technique	ALD	Sputtering	
Thickness (nm)	15	15	200
Deposition temperature (°C)	120	300	250
Resistivity ( $\mu\Omega \cdot \text{cm}$ )	6576	2847	4614
Sheet resistance ( $\Omega/\square$ )	4384	1898	307
Conductivity (S/cm)	152	351	217
			5882

**Table S2.** Resistance values obtained from modeling the impedance data in Figs. 5 and S6 with the equivalent circuit in Fig. S7(a) for as-made and S7(b) for cycled electrodes.

SiNWs	ALD1TiN /SiNWs	ALD5TiN /SiNWs	ALD15Ti N/SiNWs	Sp5TiN /SiNWs	Sp15TiN/ SiNWs
<b>As-made electrodes</b>					
$R_{el} (\Omega)$	2.3	3.5	3.9	3.4	3.5
$R_{ct} (\Omega)$	403.5	117.3	126.2	172.7	114.3
<b>Cycled electrodes</b>					
$R_{el} (\Omega)$	8.8	6.9	5.2	6.7	5.6
$R_f (\Omega)$	13.7	16.3	10.5	21.6	12.1
$R_{ct} (\Omega)$	39.4	25.5	23.5	24.8	37.9
					48.2

### Calculation of maximum volume expansion accommodated by TiN

From the TiN's Young's modulus  $E = 450 \text{ GPa}^{75}$ , the theoretical yield strength of TiN can be estimated as 40 GPa. Hence, according to Hook's law ( $\sigma = E \cdot \varepsilon$ ) a nanocrystalline TiN layer can reach a maximum yield strain of ~9%. The thickness of the nanocrystalline TiN coating is much smaller than the diameter of Si core and it is therefore reasonable to assume that the deformation of the TiN coating is uniform due to the volume expansion of Si core. If we assume there is no dis-bonding between the Si core and the TiN coating during expansion,

then the maximum radial expansion for the TiN shell and thereby SiNW core is 0.09, i.e.  $\varepsilon_r = 0.09$ . Considering Poisson's ratio of 0.25 for TiN, the length change for TiN is -0.0225, i.e.  $\varepsilon_L = -0.0225$ . As  $\varepsilon_L = \frac{L_2 - L_1}{L_1}$  and  $\varepsilon_r = \frac{r_2 - r_1}{r_1}$ ,  $L_2 = 0.9775L_1$  and  $r_2 = 1.09r_1$ . Similarly volumetric strain is defined as  $\varepsilon_V = \frac{V_2 - V_1}{V_1}$ ,  $V_1 = \pi r_1^2 L_1$  and  $V_2 = \pi r_2^2 L_2 = \pi(1.09)^2 r_1^2 (0.9775)L_1$ . Therefore, the volume change  $\varepsilon_V$ , for the Si core due to the maximum (up to 9%) elastic expansion of TiN outer layer will be ~16%. However, since we get capacity close to the theoretical specific capacity of silicon (3590 mAh/g), which corresponds to  $\text{Li}_{15}\text{Si}_4$  formation and about 280% volume change, the TiN coating should be cracking to be able to accommodate such a huge volume change.